

Rotational Brownian motion;
Fluorescence correlation spectroscopy;
Photobleaching and FRET

David A. Case
Rutgers, Spring 2010

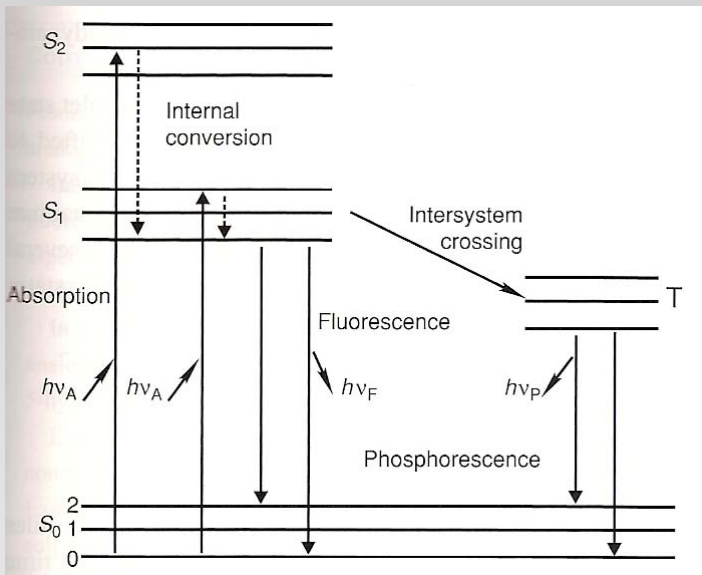
Techniques based on rotational motion

What we studied last time probed translational diffusion. There is another set of experiments that see size and shape through the lens of rotational motion. We can still use the Einstein-Sutherland equation $D = k_B T / f$, where now D and f are rotational diffusion and friction coefficients. A big difference here, though, is that there are no concentration gradients for rotational motion.

In isotropic solution, all orientations are equally likely, and something must be done to observe rotational diffusion. As with translation, there are two broad categories of experiments. In one, the initial distribution is perturbed, creating a non-isotropic distribution of molecular orientations. Then the decay back to equilibrium is analyzed. In the second set of experiments, a force is applied to achieve partial orientation, and we solve an equilibrium problem where the external torque (which creates an oriented sample) is balanced by rotational diffusion (which tends to destroy such orientation).

The first category includes **fluorescence depolarization** (Chap. D8) and **NMR relaxation** (coming later); the second includes **electric birefringence** (Chap. D6) and **flow birefringence** (Chap. D7).

Basics of fluorescence



Polarization in rigid systems

Consider a rigid, isotropic sample. The probability of finding a molecule with its transition dipole pointing the θ, ϕ direction is proportional to $\sin\theta d\theta d\phi$. Now excite this with light polarized along the z direction: the excitation probability is proportional to $|\boldsymbol{\mu} \cdot \mathbf{E}|^2$, or to $\cos^2\theta$. Thus, the distribution of excited molecules will go like $\cos^2\theta \sin\theta d\theta d\phi$. Normalizing this, we can write the distribution of excited states as

$$W(\theta, \phi, t) = \left[(3/4\pi) \cos^2\theta \sin\theta d\theta d\phi \right] \exp(-t/\tau_F)$$

At a subsequent time, the molecule may emit (fluoresce). Because the excited molecules are anisotropic, the emitted radiation will also be anisotropic. The emitted radiation polarized along z will be

$$I_{\parallel} \propto \iint \cos^2\theta W(\theta, \phi, t) d\theta d\phi = (3/4\pi) \exp(-t/\tau_F) \iint \cos^4\theta \sin\theta d\theta d\phi = (3/5) \exp(-t/\tau_F)$$

Radiation polarized on x (or along y) will be

$$I_{\perp} \propto \iint \sin^2\theta \cos^2\phi W(\theta, \phi, t) d\theta d\phi = (3/4\pi) \exp(-t/\tau_F) \iint \cos^2\phi \cos^2\theta \sin^3\theta d\theta d\phi = (1/5) \exp(-t/\tau_F)$$

Fluorescence polarization: time dependence

There are two conventional ways to express this, as **polarization** or as **anisotropy**:

$$P = (I_{\parallel} - I_{\perp}) / (I_{\parallel} + I_{\perp}); \quad A = (I_{\parallel} - I_{\perp}) / (I_{\parallel} + 2I_{\perp})$$

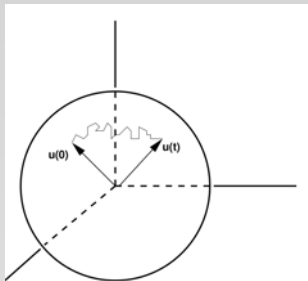
If there is no motion, then $P(0) = 1/2$ and $A(0) = 2/5$. If the emission dipole moment is aligned at a angle ξ relative to the absorption dipole, so that $\cos \xi = \mu \cdot \mu'$, then

$$P = (3 \cos^2 \xi - 1) / (\cos^2 \xi + 3); \quad A = (3 \cos^2 \xi - 1) / 5 = (2/5) P_2(\cos \xi)$$

Now, for a **non-rigid** system, if we measure the time dependence of polarization of fluorescence, it will look like a time correlation function:

$$A(t) = (2/5) \langle P_2(\mu(0) \cdot \mu(t)) \rangle \exp(-t/\tau_F) = (2/5) \langle P_2(\cos \xi(t)) \rangle \exp(-t/\tau_F)$$

Rotational diffusion



In a liquid, the molecule will suffer many small reorienting collisions with the solvent molecules, and hence \mathbf{u} should execute a “random walk” on the surface of the unit sphere. Let $f(\mathbf{u}, t)$ be the probability density of having a molecule with orientation \mathbf{u} at time t ; hence $f(\mathbf{u}, t) \sin\theta d\theta d\phi$ is the fraction of molecules in the solid angle $\sin\theta d\theta d\phi$. Debye proposed a diffusion equation:

$$\frac{\partial}{\partial t} f(\mathbf{u}, t) = D \nabla^2 f(\mathbf{u}, t) \quad (1)$$

Let's use spherical polar coordinates (r, θ, ϕ) , where $r = 1$. The Laplacian operator is then

$$\nabla^2 = \frac{1}{\sin^2\theta} \left[\sin\theta \frac{\partial}{\partial\theta} \left(\sin\theta \frac{\partial}{\partial\theta} \right) + \frac{\partial^2}{\partial\phi^2} \right] \equiv -\hat{I}^2 \quad (2)$$

$$\boxed{\frac{\partial}{\partial t} f(\mathbf{u}, t) = -D \hat{I}^2 f(\mathbf{u}, t)} \quad (3)$$

Solving the rotational diffusion problem

The formal solution of this differential equation is easily written down:

$$f(\mathbf{u}, t) = \exp(-Dt\hat{l}^2)f(\mathbf{u}, 0) \quad (4)$$

They can be written in terms of the eigenfunctions of \hat{l}^2 , which are the spherical harmonics:

$$\hat{l}^2 Y_{lm}(\mathbf{u}) = l(l+1)Y_{lm}(\mathbf{u}) \quad (5)$$

$$\exp(-Dt\hat{l}^2)Y_{lm}(\mathbf{u}) = \exp(-l(l+1)Dt)Y_{lm}(\mathbf{u})$$

The particular solution to Eq. 3 we want here corresponds to an initial condition where \mathbf{u} is sharply peaked at \mathbf{u}_0 :

$$f(\mathbf{u}, 0) = \left(\frac{1}{4\pi}\right) \delta(\mathbf{u} - \mathbf{u}_0) = \left(\frac{1}{4\pi}\right) \sum_{lm} Y_{lm}(\mathbf{u}_0) Y_{lm}^*(\mathbf{u}) \quad (6)$$

where the final equality exploits the closure relation of the spherical harmonics. Combining this with Eq. 4 gives:

$$f(\mathbf{u}, t) = \sum_{lm} \exp(-l(l+1)Dt) Y_{lm}(\mathbf{u}_0) Y_{lm}^*(\mathbf{u}) \quad (7)$$

Time-correlation functions

The time-correlation functions needed for NMR relaxation only require the second moments of this distribution. If $F_n(\mathbf{u}) \sim (4\pi/5)^{1/2} Y_{2n}(\mathbf{u})$:

$$\begin{aligned}\langle F_n(\mathbf{u}_0)F_n^*(\mathbf{u}) \rangle &\sim \left(\frac{1}{4\pi}\right) \int d^2u_0 \int d^2u \left[\frac{4\pi}{5}\right] Y_{2n}(\mathbf{u}_0)Y_{2n}^*(\mathbf{u}) \\ &= \left(\frac{1}{5}\right) \exp(-6D\tau)\end{aligned}$$

Hence, for a rigid molecule undergoing such isotropic Brownian rotational motion, the normalized F_n time-correlation functions for all internuclear vectors all decay in the same way, as

$$C^{rot}(\tau) = \langle P_2(\mathbf{u}_0 \cdot \mathbf{u}) \rangle = \sum_{n=-2}^{n=2} \langle F_n(\mathbf{u}_0)F_n^*(\mathbf{u}) \rangle = \exp(-\tau/\tau_c) \quad (8)$$

where the time constant τ_c is $1/6D = V_h\eta/k_B T$. (For later): its Fourier transform is then a Lorentzian:

$$j^{rot}(\omega) \equiv \frac{2}{5} \int_0^\infty (\cos \omega t) C(t) dt = \left(\frac{2}{5}\right) \frac{\tau_c}{1 + \omega^2 \tau_c^2} \quad (9)$$

Dynamics of Mismatched Base Pairs in DNA[†]

Christopher R. Guest,[‡] Remo A. Hochstrasser,[‡] Lawrence C. Sowers,[§] and David P. Millar^{*;‡}

Department of Molecular Biology, Research Institute of Scripps Clinic, La Jolla, California 92037, and Division of Pediatrics, City of Hope National Medical Center, Duarte, California 91010

Received July 10, 1990; Revised Manuscript Received December 12, 1990

ABSTRACT: The structural dynamics of mismatched base pairs in duplex DNA have been studied by time-resolved fluorescence anisotropy decay measurements on a series of duplex oligodeoxynucleotides of the general type d[CGG(AP)GGC]-d[GCCXCCG], where AP is the fluorescent adenine analogue 2-aminopurine and X = T, A, G, or C. The anisotropy decay is caused by internal rotations of AP within the duplex, which occur on the picosecond time scale, and by overall rotational diffusion of the duplex. The correlation time and angular range of internal rotation of AP vary among the series of AP·X mismatches, showing that the native DNA bases differ in their ability to influence the motion of AP. These differences are correlated with the strength of base-pairing interactions in the various AP·X mismatches. The interactions are strongest with X = T or C. The ability to discern differences in the strength of base-pairing interactions at a specific site in DNA by observing their effect on the dynamics of base motion is a novel aspect of the present study. The extent of AP stacking within the duplex is also determined in this study since it influences the excited-state quenching of AP. AP is thus shown to be extrahelical in the AP·G mismatch. The association state of the AP-containing oligodeoxynucleotide strand is determined from the temperature-dependent tumbling correlation time. An oligodeoxynucleotide triplex is formed with a particular base sequence in a pH-dependent manner.

Absorption and emission spectra

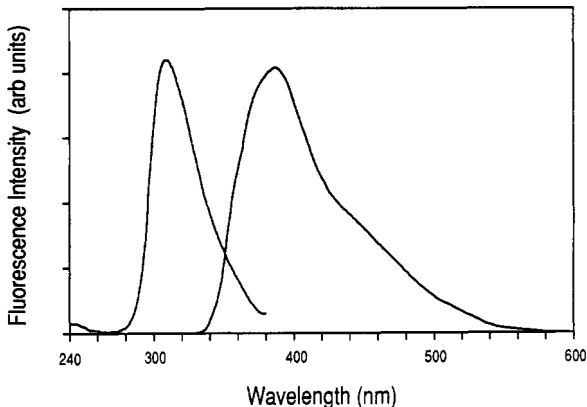


FIGURE 3: Steady-state fluorescence excitation (at left) and emission (at right) spectra of 50 μM d[CGG(AP)GGC]-d[GCCTCCG] in 50 mM Tris-HCl, pH 7.4, and 0.15 M NaCl at 20 $^{\circ}\text{C}$. In the excitation spectrum, the emission is observed at 380 nm, while in the emission spectrum the excitation wavelength is 320 nm. The band-pass is 5 nm for both excitation and emission.

Time-dependence of polarization:

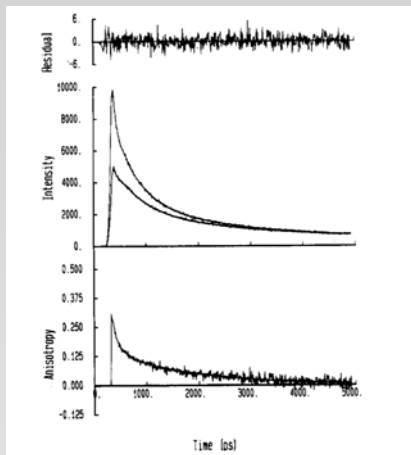


FIGURE 4: Time-resolved emission depolarization of d[CGG(AP)-GGC]-d[GCCGCCG] in 50 mM Tris-HCl, pH 7.4, and 0.15 M NaCl at 4 °C. The center panel shows the polarized emission intensities $I_{\parallel}(t)$ (upper curve) and $I_{\perp}(t)$ (lower curve). The time-dependent emission anisotropy is shown in the lower panel. The smooth lines are best-fit curves generated as described in the text. The upper panel shows the weighted deviation between the experimental difference curve, $I_{\parallel}(t) - I_{\perp}(t)$, and the best-fit difference curve.

Fitting the data

Table II: Anisotropy Decay Parameters^a

X^b	T (°C) (±0.5)	τ_{r1} (ps) (±15)	τ_{r2} (ns) (±0.07)	r_{01} (±0.015)	r_{02} (±0.015)	r_0 (±0.030)
T	40	60	0.50	0.210	0.127	0.337
	30	73	0.65	0.229	0.127	0.356
	20	85	0.80	0.227	0.117	0.344
	10	100	1.10	0.235	0.106	0.341
	4	124	1.70	0.249	0.099	0.348

$$A(t) = (2/5) [S^2 + (1 - S^2) \exp(-t/\tau_i)] \exp(-t/\tau_c)$$

Table III: Correlation Time, Order Parameter, and Cone Angle for Restricted Motion of 2-Aminopurine^a

X^b	T (°C) (±0.5)	τ_i (ps) (±15)	S (±0.070)	θ_0 (deg) (±3)
T	40	68	0.614	44
	30	82	0.597	45
	20	95	0.583	46
	10	110	0.558	48
	4	135	0.533	50

Steady-state fluorescence polarization

Instead of measuring the time-dependence of polarization, it is usually easier to look at the averages, or steady-state values under constant illumination:

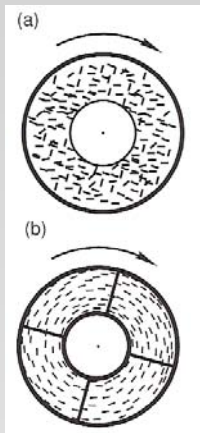
$$\langle I_{\parallel} \rangle = \tau_F^{-1} \int_0^{\infty} I_{\parallel}(t) dt; \quad \langle I_{\perp} \rangle = \tau_F^{-1} \int_0^{\infty} I_{\perp}(t) dt$$

Note that the amount of depolarization will depend on the ratio of τ_c (how fast the molecule tumbles) to τ_F (how long it takes on average to fluoresce. Plugging our previous values in (ignoring internal motion for simplicity for now):

$$\langle A \rangle^{-1} = (5/2)(1 + \tau_F/\tau_c) = (5/2)(1 + \tau_F k_B T / V_h \eta)$$

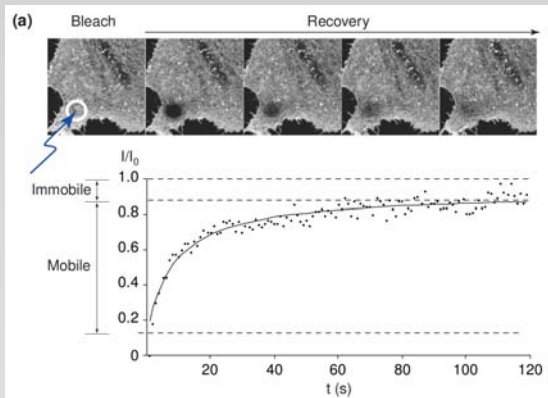
This is called the **Perrin equation**.

Orientation by flow birefringence



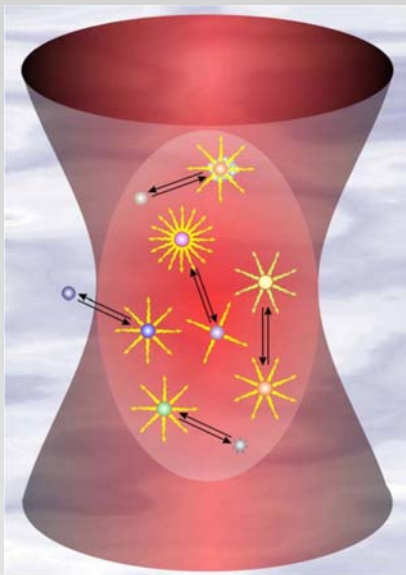
Another way to create an anisotropic distribution of orientations is illustrated here. Under a flow, molecules will tend to orient along the flow direction. As with sedimentation, one can do an equilibrium experiment (pp. 438-439), where the external torque coming from the velocity gradient matches rotational diffusion. Or, one can do a time-dependent experiment where the flow is abruptly turned off, and the decay back to equilibrium is measured (pp. 440-441).

Photobleaching and recovery



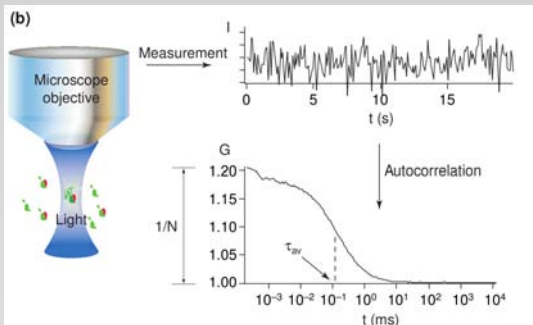
Fluorescence recovery after photobleaching (FRAP) is based on photobleaching the fluorescent protein within a small region of interest (ROI) in the cell (white circle) by short, high-intensity laser illumination. Subsequent exchange between the bleached and non-bleached populations of fluorescent protein in the ROI is monitored by quantitative time-lapse microscopy and the fluorescence intensity relative to the pre-bleach period (I/I_0) is plotted as a function of time. Curve fitting (solid line) can then be used to determine the effective diffusion coefficient $Deff$ and the mobile and immobile fractions of protein.

Fluorescence correlation spectroscopy



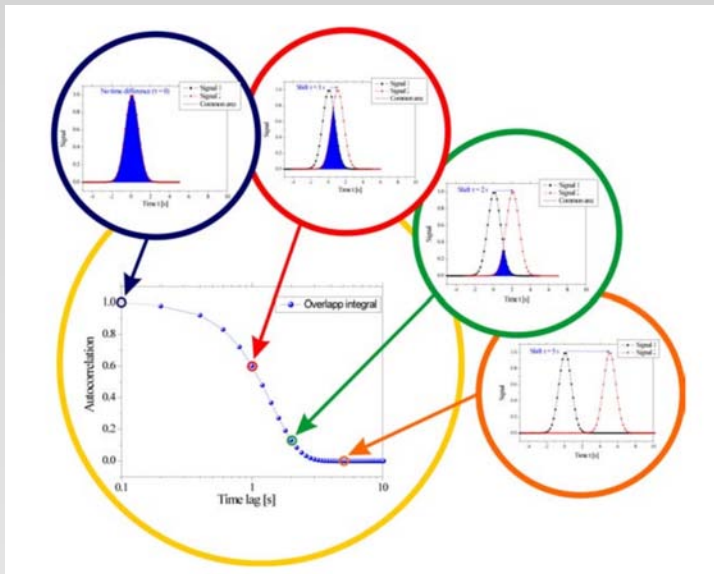
Here we use fluorescence to study fluctuations in fluorescence intensity in small volumes. Molecular mechanisms that might give rise to fluorescence fluctuations include particle movements, conformational changes, chemical or photophysical reactions. The key is to have only a small number of molecules in the observation volume, since the relative size of fluctuations goes like $N^{-1/2}$. Here, volume is about 10^{-15} liter. Concentration is between nanomolar and micromolar. Hence the number of particles in the viewing volume is between 0.1 and 1000.

Experimental setup and basic ideas

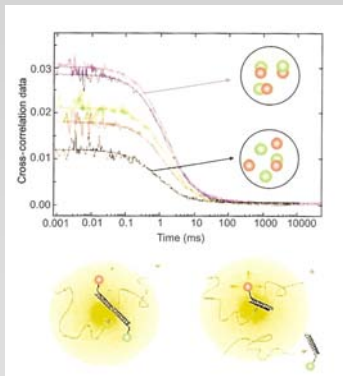


In fluorescence correlation spectroscopy (FCS) a small, geometrically defined light cavity (with a volume smaller than 1 femtoliter) is generated in the sample by confocal illumination. Only very few tagged proteins are emitting fluorescent light in this cavity at any particular time. The fluctuations in the fluorescence signal are recorded (horizontal arrow), from which the autocorrelation function is computed (vertical arrow). The fluctuations are caused by diffusion of fluorescent molecules through the cavity or by changes in fluorescence over time caused by chemical reaction kinetics. From the autocorrelation function the average dwell time (τ_{av}) and number of molecules in the cavity (N) can be derived. Together with the known size of the light cavity, this can then be used to determine the diffusion coefficient D of the fluorescent probe.

Development of an autocorrelation curve



Two-color fluorescence correlations



D can then be used to evaluate the formation of molecular complexes as the diffusion of molecular complexes (red and green structures) is slower than that of free protein molecules (green structures) resulting in a smaller value for D . Chemical reaction-specific fluctuations are independent of the size of the light cavity, in contrast to diffusion-controlled processes. By changing the size of the light cavity, the rate constants of protein reaction kinetics can be discriminated from the dwell time of molecules in the light cavity.

Diffusion analysis in cells

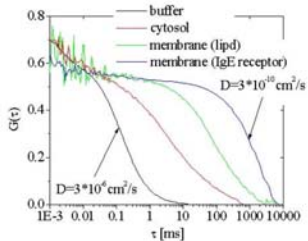
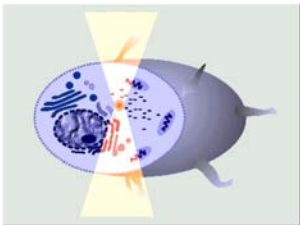
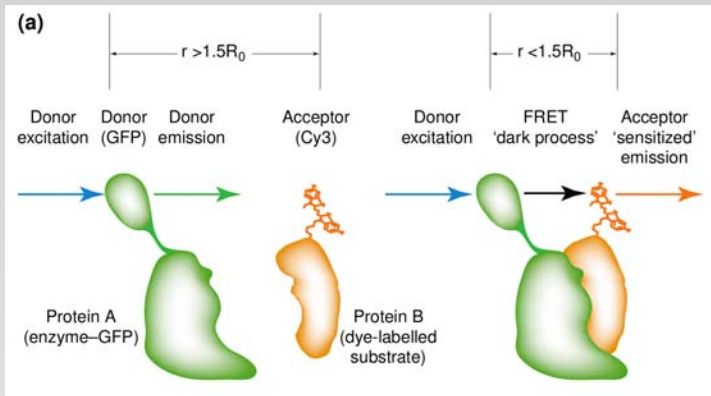


Figure 15: Various autocorrelation curves demonstrating the enormous difference in motility between buffer solution and cytosol

Fluorescence resonant energy transfer



Fluorescence resonance energy transfer (FRET) is a non-radiative process whereby energy from an excited donor fluorophore is transferred to an acceptor fluorophore that is within nanometre range. FRET is useful as a photophysical phenomenon to measure protein interactions as the efficiency E at which Förster-type energy transfer occurs is steeply dependent on the distance r (nm) between the two fluorophores is given by: $R_0^6 / (R_0^6 + r^6)$, where R_0 is typically between 2 and 6 nm.

Fluorescence resonant energy transfer

(b)

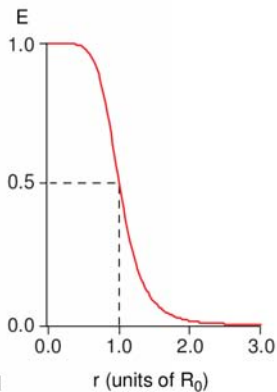
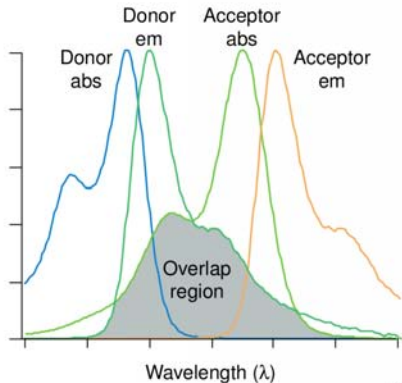


Figure 1

(c)



TiBS